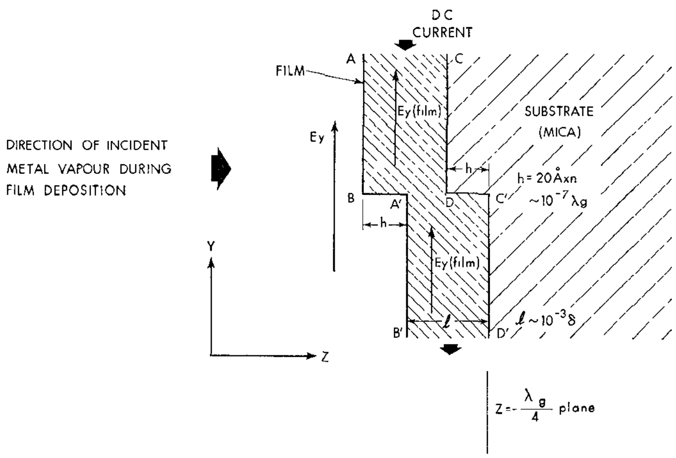

Fig. 4.

II. Experimental Results

Measurements were made at 9700 ± 2 MHz in X-band waveguide for which $Z_0 = 511.8\Omega$ for gold and gold–silver films deposited by high-vacuum evaporation on air-cleaved mica sheets with $d \leq 0.03$ mm and mounted as shown in Fig. 1 [9]. The film dimensions between the silver contact strips were 1 by 1/2 in, giving two squares in parallel. Thus twice the dc resistance (measured to within ± 1-percent accuracy) gives R_s. In practice, even with a mica sheet on both sides of the film, there is sufficient capacitive coupling between the contact strips and the broadside waveguide walls for the film to act essentially as a conductance across the waveguide [10].

The discontinuity was assessed using the sliding load technique [11]. The VSWR of the holder without a mica sheet was 1.035 (corresponding to a reflection coefficient $|\Gamma_1| = 0.017$). With a 0.03-mm thick mica sheet, the VSWR increased to 1.056 ($|\Gamma_2| = 0.027$). Considering Γ_1 and Γ_2 in phase, $\Gamma_e = 0.01$ and $r_e = 1.02$, which closely agrees with the value 1.0124 calculated from (1). The maximum error, at $R_s(\mu) = Z_0$, is then found to be ± 2 percent if r_e is ignored. As the VSWR can be measured to within 2 percent for $r \leq 10$, the total error is less than ± 5 percent for $50 \leq R_s(\mu) < 5000\ \Omega/\square$.

The measured values of $R_s(\mu)$, R_s, ρ_μ, and dc resistivity $\rho_0 (= lR_s)$, the last two normalized to the bulk resistivity of gold ($\rho_G = 2.44 \times 10^{-6}$ $\Omega \cdot$cm), are shown in Fig. 2 and 3.

III. Discussion

No direct correlation between R_s and $R_s(\mu)$ has been found. Fig. 2 suggests that for R_s below about 40 $\Omega/\square$, $R_s(\mu)$ is generally greater than R_s; there are some points where $R_s(\mu) \simeq R_s$; otherwise, $R_s(\mu)$ is generally smaller than R_s. These factors are further emphasized in Fig. 3 where a transition from $\rho_0/\rho_G < \rho_\mu/\rho_G$ to $\rho_0/\rho_G > \rho_\mu/\rho_G$ is seen to occur for l around 80 Å. At 50 Å, ρ_0/ρ_G is about three times larger than ρ_μ/ρ_G, a difference far beyond the limits of experimental error.

Waveguide losses and an imperfect short circuit are likely to reduce the measured value of r. Thus when $R_s(\mu) = rZ_0$, $R_s(\mu)$ will be smaller than R_s; for the case when $R_s(\mu) = Z_0/r$, $R_s(\mu)$ will be larger than R_s. For the former case, however, l is less than about 80 Å and a much more important factor is the surface microtopography of the substrate. Carefully cleaved mica sheets, although atomically smooth over large areas, still exhibit a hill-and-valley topography, and cleavage-step heights h are known to be $\sim$20 Å or integral multiples thereof [7]. Fig. 4 shows an idealized cross section of a film with l slightly larger than h and no deposition on the step. The resulting constricted area through $A'D$ forms a higher resistivity path for dc, and a multiplicity of such defects would considerably increase the measured R_s value. E_y, however, is essentially the same at faces AB and $A'B'$ since $h \sim 10^{-7}\ \lambda_g$. Also, E_y (film) and the resulting film current density σE_y (film) are uniform over l, since $l \leq 10^{-3}\ \delta$. Surface undulations further lengthen the dc path. At microwave frequencies, on the other hand, Ament [12] has shown that an approximate value of the reflection coefficient of a perfect conductor with statistically distributed surface irregularities is $\exp\left(-2k^2\overline{h^2}\sin^2\theta\right)$, where $k^2 = \omega^2\mu_0\epsilon_0$, $\overline{h^2}$ is the mean-square height of the irregularities, and θ is the angle of incidence of the wave. This is almost unity for $\overline{h^2} \ll \lambda^2$. The result of microscopic surface irregularities on $R_s(\mu)$ measurements must therefore be minimal. The dc resistivity calculated using macroscopic film geometry is meaningless as l approaches h or $(\overline{h^2})^{1/2}$, particularly because no two cleavage faces will be the same.

References

[1] J. C. Slater, *Microwave Electronics*. Princeton, N. J.: Van Nostrand, 1950, pp. 34–35.
[2] D. E. Clark, "The resistivity of thin metallic films," *Brit. J. Appl. Phys.*, vol. 6, pp. 158–160, May 1955.
[3] K. S. Champlin, J. D. Holm, and G. H. Glover, "Electrodeless determination of semiconductor conductivity from TE_{01}°-mode reflectivity," *J. Appl. Phys.*, vol. 38, pp. 96–98, Jan. 1967.
[4] R. L. Ramey and T. S. Lewis, "Properties of thin metal films at microwave frequencies," *J. Appl. Phys.*, vol. 39, pp. 1747–1752, Feb. 1968.
[5] H. H. Wieder, *Intermetallic Semiconductor Films*. London, England: Pergamon, 1970, pp. 180–187.
[6] R. H. Havemann and L. E. Davis, "Conductivity and the microwave properties of 81-permalloy thin films," *IEEE Trans. Microwave Theory Tech.* (Corresp.), vol. MTT-19, pp. 113–116, Jan. 1971.
[7] S. Tolansky, *Microstructure of Surface using Interferometry*. New York: American Elsevier, 1968, pp. 15–17.
[8] T. Moreno, *Microwave Transmission Design Data*. New York: Dover, 1958, p. 170.
[9] H. K. Chaurasia, "Studies on thin films of gold," M.A.Sc. thesis, Dep. Elec. Eng., Univ. of British Columbia, Vancouver, Canada, Oct. 1964.
[10] B. M. Schiffmannm, L. Young, and R. B. Larrick, "Thin-film waveguide bolometers for multimode power measurements," *IEEE Trans. Microwave Theory Tech.*, vol. MTT-12, pp. 155–163, Mar. 1964.
[11] *Microwave Measurements for Calibration Laboratories*, Hewlett-Packard Application Note 38, Section 4, p. 11, 1962.
[12] W. A. Ament, "Toward a theory of reflection by a rough surface," *Proc. IRE*, vol. 41, pp. 142–146, Jan. 1953.

Compact YIG Bandpass Filter with Finite-Pole Frequencies for Applications in Microwave Integrated Circuits

PETER RÖSCHMANN

***Abstract*—A miniaturized, narrow-bandwidth, two-stage YIG bandpass filter is described that can be incorporated into microstrip circuits. The selectivity is increased by introducing finite-pole frequencies. This is realized by additional coupling between the input and output lines leading to the YIG-coupling section.**

The problem of achieving high selectivity in microwave integrated circuits (MIC's) has not really been solved for reasons that microstrip is too lossy, dielectric resonators are temperature sensitive, and cavity resonators are too large. This short paper describes a fixed, tuned, YIG bandpass filter with permanent magnets that satisfies the conditions required for narrow-bandwidth filters in MIC's: small size, tolerable losses, and temperature stability.

Although single-crystal YIG sphere resonators [1][1] with typical diameters between 0.3 and 1 mm are compatible in size with microstrip lines that have a substrate thickness and stripline width of the same order, a hybrid integration of the YIG filter into the MIC was preferred to a full integration of the YIG sphere resonators into the microstrip substrate. There are several reasons that lead to the preference of a hybrid integration: 1) the biasing magnet, which in any case must be built around the YIG filter; 2) difficulties in realizing a planar coupling structure for YIG bandpass filters in only one plane, as given by the circuit plane of the substrate; and 3) the adjustments and tests of the YIG filter are more easily made in a test jig than in a more or less complex microwave circuit.

Therefore, the YIG filter was designed as a separate miniaturized component which, like a transistor or a diode, can be built into the appropriate part of the MIC. Fig. 1 shows the miniaturized YIG filter as a separate component and the YIG filter component connected to a microstrip substrate (seen from the ground plane side and from the circuit side of the substrate). An area of only 8×5 mm² is needed on the circuit plane of the substrate for mounting and connecting the filter. The filter is a two-stage type consisting of two orthogonal semiloop coupling structures; the permanent magnet sys-

Manuscript received October 19, 1971; revised July 6, 1972.
The author is with Philips Forschungslaboratorium, Hamburg 54, Germany.
[1] In [1], the general properties of YIG resonators are described.

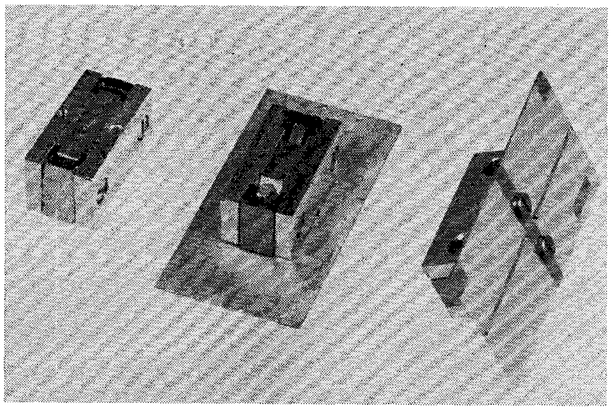

Fig. 1. The miniaturized YIG filter as a separate component (left side) and as connected to a 1×1/2-in microstrip substrate seen from the ground plane side (middle) and from the circuit side (right).

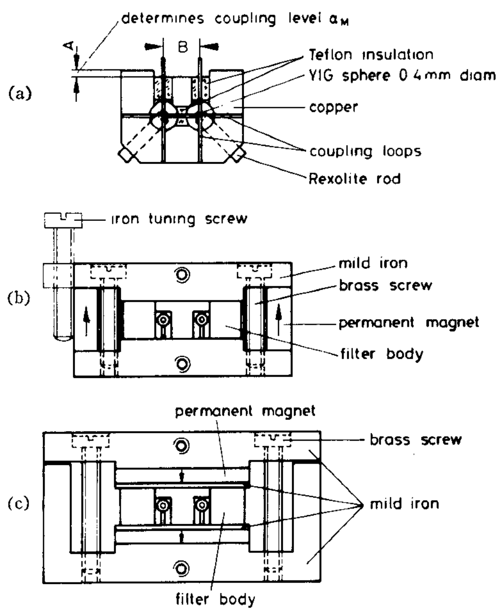

Fig. 2. Sketch of the compact YIG bandpass filter. (a) Filter body. (b) Assembled filter component indicating arrangement for magnetic shunt tuning. (c) Magnet system offering shielding against external fields.

tem is made from Philips Ticonal 450 and a mild iron yoke. Fig. 2 (a) and (b) shows design details of the filter body and the assembled filter component, respectively. The data of this filter are given below:

center frequency f_0	2500 MHz
3-dB bandwidth	12 MHz
insertion loss	1.7 dB
temperature sensitivity of f_0 from 20°C to 70°C	$< \pm 1$ MHz
size	$12\times 6\times 5$ mm^3
RF power-limiting level for YIG spheres 0.42-mm diam	-27 dBm
same for 1000-G YGaIG spheres 0.5-mm diam	$+13$ dBm

Higher center frequencies up to X band are feasible without much increase of the magnet size by using samarium cobalt, whereas a lower frequency limit of this application is given by the decreasing unloaded Q of gallium-substituted YIG at approximately 500 MHz.

In order to obtain a stable operation of the filter over temperature with respect to insertion loss and the center frequency, the magnetic field at the positions of the YIG spheres must be identical and homogeneous. This was achieved by using a mild iron with high permeability for the yokes and by assuring a parallelity of the pole faces within 0.01 mm over the pole area dimensions of 5 mm×7 mm. Thus the two-stage filter attenuation characteristic is preserved for temperatures ranging from at least 0°C to +70°C. A slight rise of the insertion loss of 0.1–0.2 dB with increasing temperature is mainly due to the decreasing saturation magnetization of the YIG material. This influences the RF coupling of the YIG spheres and results in a 10-percent decrease of the 3-dB bandwidth over the measured temperature range.

Techniques to render the resonant frequency of a YIG sphere insensitive to temperature by compensating the anisotropy field with proper crystallographic orientation are well known for constant tuning fields [2]. However, the permanent magnets used have a temperature coefficient of the remanent magnetization of approximately −0.01 percent/°C. Due to the crystal anisotropy field, YIG spheres can be oriented to show a negative, zero, or positive temperature coefficient of the resonant frequency, which allows a compensation of the temperature drift given by the permanent magnet. By these means, a positive or negative drift of the center frequency of 0.5–1 MHz over a temperature range from 20°C to 70°C was achieved experimentally with different filters.

The unshielded construction of the magnet system of Fig. 2(b) makes the filter sensitive to external magnetic fields and to magnetic materials in the vicinity. This results in a shift of the center frequency, but due to the parallel pole faces the attenuation characteristic and the insertion loss remain unchanged. Therefore, an adjustable magnetic shunt at the outside of one or both of the permanent magnets provides a simple method for tuning the filter. A single iron screw of 1-mm diam and 6-mm length, as indicated in Fig. 2(b), gives a tuning range of 100 MHz. More than 500 MHz tuning has been obtained by using stronger shunts on both sides of the magnet.

The earth's magnet field also influences the center frequency, resulting in a frequency shift up to ±1.6 MHz depending on the relative position of the YIG filter. This value fairly agrees with the measured value of 0.4 Oe in the surrounding of experimentation and including the field enhancement due to the yokes.

The leakage or stray fields of the magnet system limit the packaging density of the described filter. A frequency shift of 2 MHz was observed for a distance of 1 cm between two filters. Other parts like circulators, isolators, etc., made of magnetic material begin to influence the center frequency of the filter at a distance of 5 cm–10 cm depending on size and the magnitude of the magnetic leakage fields. However, provided the "magnetic environment" of the filter can be regarded stationary in space and time, then a final passband frequency of the filter *in situ* can be adjusted by the magnetic shunt method.

An improvement regarding the effects of external magnetic parts or fields is obtained by using a magnet system according to Fig. 2(c), however, at the expense of size, simplicity, and decreased tuning capability. Due to the stronger demagnetization of the flat permanent magnets, materials with a high coercive field, like samarium cobalt or platinum cobalt, must be used.

The skirt selectivity of a filter (Butterworth or Chebyshev characteristic) with a given number of stages can be increased by finite-pole frequencies (elliptic function or Cauer filter, n-path filter). We have obtained pole frequencies in YIG filters by introducing a weak RF magnetic coupling between the input and output line leading to the YIG-coupling section. This technique is incorporated into the miniaturized two-stage YIG filter of Fig. 1. The wall between the input and output line is partly removed as shown in Fig. 2(a) to achieve the required coupling, and a typical response is shown in Fig. 3.

A simplified equivalent circuit of the finite-pole YIG filter is given in Fig. 4, where M indicates the magnetic coupling from the input to the output of the YIG filter. The coupling level α_M and the 3-dB bandwidth of the filter determine the position of the pole frequencies with respect to the passband center frequency. This is schematically shown in Fig. 5. The pole frequencies occur at the intersection of α_M with the all-pole response; here, the coupled signal α_M and the signal transmitted by the YIG spheres nearly cancel.

An approximate calculation of these conditions can be made if we assume a critically coupled (maximally flat) YIG filter response and neglect the insertion loss and the phase error due to the short line

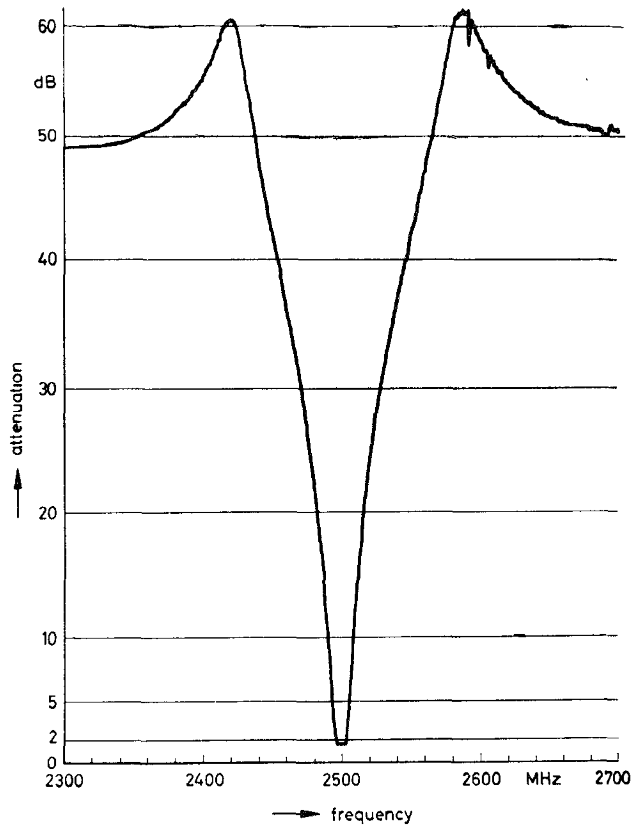

Fig. 3. Measured response of a miniaturized finite-pole frequency YIG filter; $\alpha_M = 48$ dB.

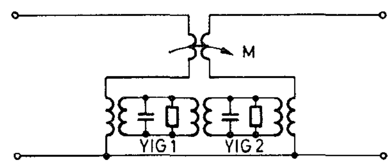

Fig. 4. Simplified equivalent circuit of a two-stage YIG bandpass filter with finite-pole frequencies.

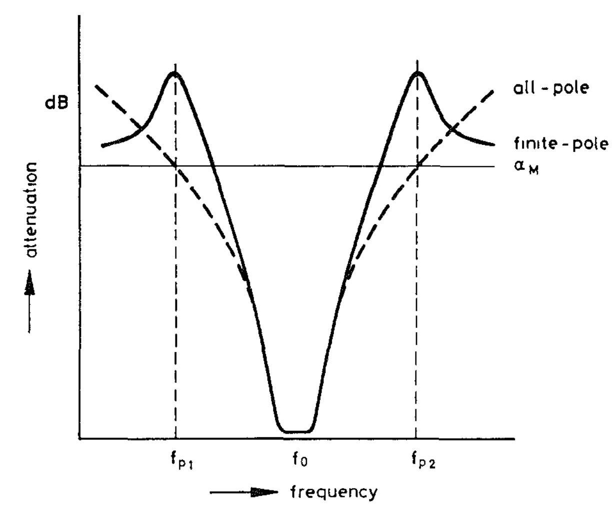

Fig. 5. All-pole and finite-pole filter responses showing the influence of the input to output port coupling level α_M (schematic).

length between the YIG-coupling section and the coupling locus for α_M. The ratio R of the voltage at the load of a maximally flat two-stage filter to the voltage across the load when directly connected to a generator is given by [3]

$$R = \frac{1}{X^2 - 1 - j\sqrt{2}X} \tag{1}$$

where X is a normalized frequency deviation according to

$$X = \frac{f_0}{\Delta f_{3\,\text{dB}}}\left(\frac{f}{f_0} - \frac{f_0}{f}\right). \tag{2}$$

If f is within 10 percent of f_0,

$$X \approx \frac{f - f_0}{\frac{1}{2}\Delta f_{3\,\text{dB}}}. \tag{2a}$$

Note that the phase of R at the center frequency ($X=0$) is equal to π and not zero as it should be. This is due to the particular way in which [3, eq. (1)] has been derived. However, for our purpose this equation is used, since each of the orthogonal loop-coupled YIG spheres produces at resonance a phase shift of $\pm\pi/2$, giving a total phase shift of $(\pm)\pi$.

The analogous equation of the voltage ratio R_P of the finite-pole filter becomes, after rewriting (1) and neglecting for $X \to 0$, the influence of the filter on α_M:

$$R_P \approx \frac{X^2 - 1}{X^4 + 1} + j\frac{\sqrt{2}\cdot X}{X^4 + 1} - \frac{1}{A_M} \tag{3}$$

which can be further simplified since we are only interested in values $X \gg 1$:

$$R_P \approx \frac{1}{X^2} - \frac{1}{A_M} + j\frac{\sqrt{2}}{X^3} \tag{3a}$$

where

$$A_M = \text{antilog}_{10}\frac{\alpha_M}{20} \tag{4}$$

is a voltage ratio due to the frequency independent coupling from the input to the output port of the YIG filter; the phase of this signal must be frequency independent and in phase with the signal transmitted by the YIG filter at the center frequency.

The pole frequencies are found with good approximation when the real terms of (3a) cancel at

$$X_p \approx \pm\sqrt{A_M} \tag{5}$$

and with (2a)

$$f_p - f_0 \approx \pm\sqrt{A_M}\cdot\tfrac{1}{2}\Delta f_{3\,\text{dB}}. \tag{6}$$

The argument of the imaginary part of (3a) gives the amplitude at the pole frequencies. Thus the pole attenuation α_p in decibels is obtained with (4) and (5)

$$\alpha_p \approx 1.5\,\alpha_M - 3\ \text{dB}. \tag{7}$$

A qualitative proof of (6) and (7) is found by results given in Table I, which shows measured and calculated data of several filters at $f_0 = 2500$ MHz with different values α_M.

The differences found with the pole frequencies can partly be attributed to the fact that the YIG filters did not show an exact maximal flat prototype response, but rather a pseudo-Chebyshev response due to the finite and possibly different unloaded Q (1500–2000) of the YIG spheres and unavoidable dimensional tolerances of the coupling loops, which results in an asymmetrical coupling. Thus the attenuation will be higher than assumed with (1) and the pole frequencies are situated more closely toward the center frequency. This is confirmed by the empirical approach indicated in Fig. 5. The actual measured YIG filter response has been fitted to a suitable Chebyshev prototype response characteristic in the 0–25 dB attentuation range, where the effect of α_M can be neglected. Extrapolation to α_M yields the empirical results $(f_p - f_0)$ of Table I. A 0.2-dB Chebyshev response was found

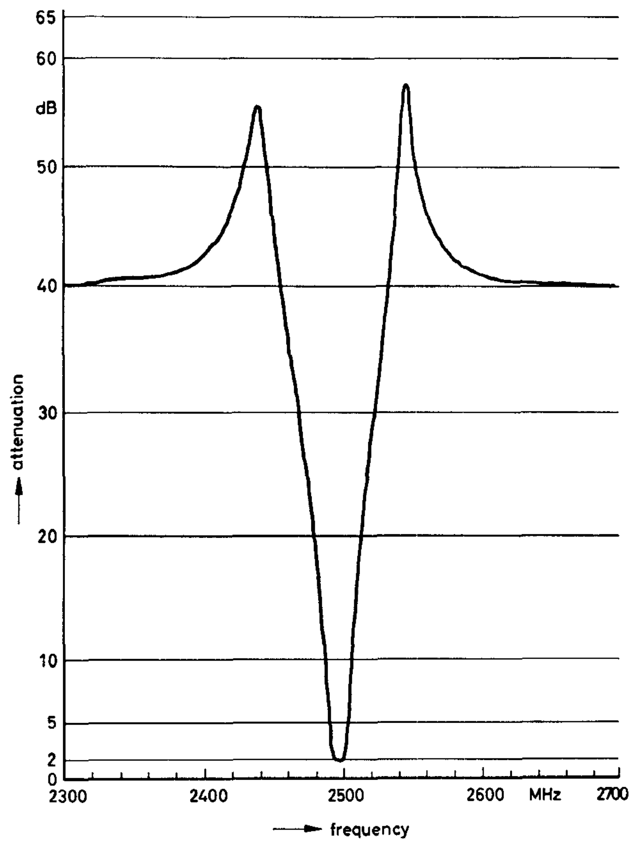

Fig. 6. Measured response of a miniaturized finite-pole frequency YIG filter; α_M =40 dB.

TABLE I

COMPARISON OF MEASURED AND CALCULATED DATA OF FINITE-POLE FREQUENCY YIG FILTERS AT 2500 MHz HAVING VARIOUS COUPLING LEVELS α_M

Δf_{3dB} (MHz)	α_M (dB)	f_o-f_{p1} (MHz)	$f_{p2}-f_o$ (MHz)	f_p-f_o eq. (6) (MHz)	f_p-f_o empirical (MHz)	α_{p1} (dB)	α_{p2} (dB)	α_p eq. (7) (dB)
12	40	56	50	60	55	55	57	57
11	45	60	65	73	67	62	58	64.5
12	48	82	88	95	87	61	62	69
11.5	51	100	90	108	98	64	64	73.5
21	50	155	165	187	167	64	60	72

suitable, which also agrees well with the VSWR of 1.4–1.8 measured at the center frequencies of the filters.

Possibly another contribution comes from the effect of the coupling inductances on the passband characteristic of a YIG filter, as has been described by Carter [4]; this effect could also partly explain the asymmetry of the pole frequencies and of the attenuation response. However, since there is no clear tendency of the measured results with this respect, other causes must also be taken into account: the frequency dependence of α_M, the short transmission-line length leading from the YIG-coupling section to the reference plane of the additional coupling α_M, also the misalignment of the orthogonal coupling loops and a YIG sphere position outside the center of the crossed coupling loops, which both lead to a nonreciprocal phase shift deviating from $\pm\pi$ due to the gyrator properties of the cascaded YIG sphere resonators. The latter effect has also been checked by measuring the filter in reverse direction. In some cases, the values of α_p at the lower and higher frequency side of f_0 are just exchanged; for other filters α_{p1} or α_{p2} or both are decreased or increased up to 3 dB, but the pole frequencies remain constant for both directions.

The agreement of the measured and calculated values α_p of Table I is quite good for the lower values of α_M. Because the YIG-coupling sections show a crosstalk of the order of 65 dB to 70 dB, which has been measured on similar two-stage filter structures without additional coupling α_M in the 2-GHz to 4-GHz range, the highest values

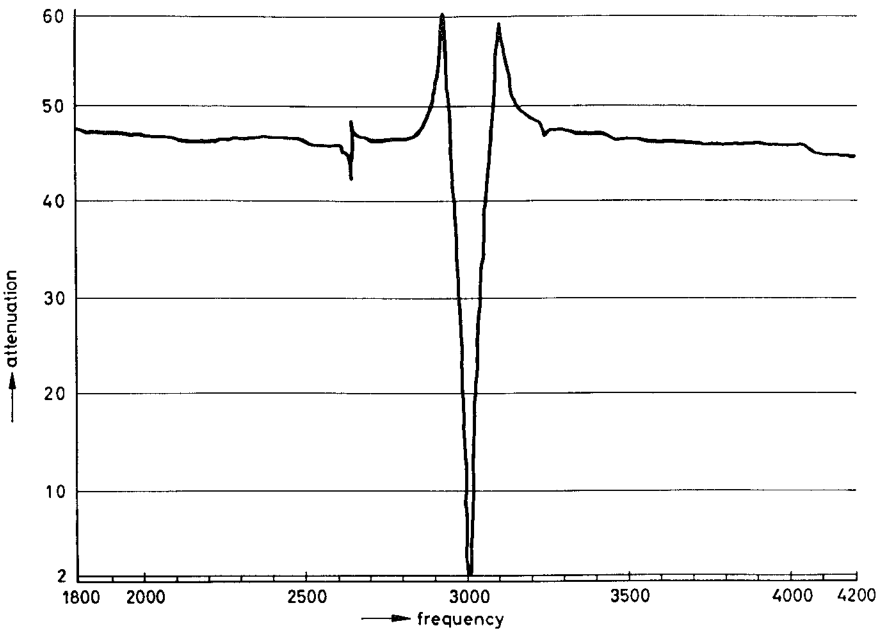

Fig. 7. Typical measured wide-band response of a finite-pole frequency YIG filter showing the frequency dependence of α_M.

TABLE II

EXPERIMENTAL RESULTS OF COUPLING LEVEL α_M AS A FUNCTION OF DIMENSION A AND B OF FIG. 2(a) BETWEEN 2 AND 4 GHz

A (mm)	B (mm)	α_M (dB)
0	2.5	50 ± 2
0.3	2.5	47 ± 1.5
0.5	2.5	45 ± 1.5
0	2.0	44 ± 2
0.3	2.0	41 ± 1.5

TABLE III

FREQUENCY DEPENDENCE OF A YIG FILTER WITH FINITE-POLE FREQUENCIES

f_o (GHz)	α_o (dB)	ripple (dB)	α_M (dB)	Δf_{3dB} (MHz)	f_o-f_{p1} (MHz)	$f_{p2}-f_o$ (MHz)	f_p-f_o eq. (6) (MHz)	α_{p1} (dB)	α_{p2} (dB)	α_p eq. (7) (dB)
2	2	1	46	19	100	110	134	64	60	66
2.5	1.8	0.6	46	20	105	115	141	63	60	66
3	1.5	0.3	45	21	110	120	140	62	59	64.5
3.5	1.5	≈0.2	45	21	110	120	140	62	58	64.5
4	1.5	≈0.2	44	22	120	130	138	61	57	63

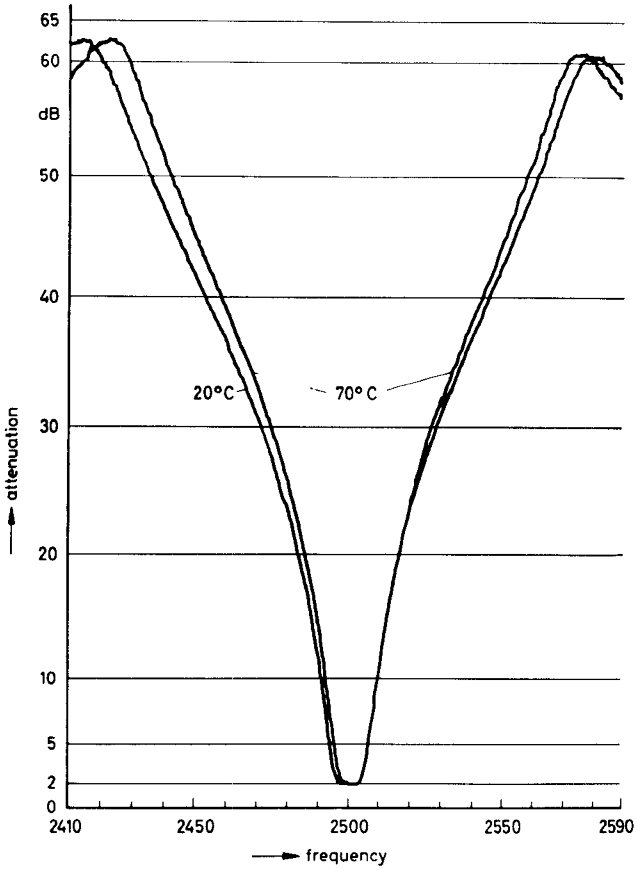

Fig. 8. Effect of operating temperature on the attenuation poles; $\alpha_M = 48$ dB.

of α_p can be expected up to 6 dB below the actual crosstalk values. This is confirmed by the results for high α_M values in Table I and explains the deviation from (7). An asymmetry of the level of α_p also partly arises if the crosstalk of each of the two YIG-coupling sections is different and if α_M is different at the pole frequencies.

Due to the crosstalk, the upper limit of α_M for applications will be of the order of 55 dB; the lower limit is mainly given by the required rejection level, but also by the reduced effectiveness according to (7). This is demonstrated in Fig. 6 for the case of $\alpha_M = 40$ dB. Measured values of the coupling level α_M at 2 GHz to 4 GHz as function of dimension A and the separation B between the center conductor of the input and output coaxial lines (Fig. 2) are given in Table II. These data were obtained using a 0.01-in Al_2O_3 substrate for the MIC and 0.2-mm diam center conductors; it is expected that the substrate thickness has a similar influence on α_M to dimension A. Higher values α_M could be realized by increasing the distance B between the input and output line.

A typical frequency dependence of α_M can be seen in Fig. 7. Due to the very smooth variation of α_M, tuning over an octave from 2–4 GHz was achieved without substantial changes in the pole attenuation characteristic. A filter of the type described was placed into a laboratory electromagnet and the permanent magnets were removed from the yokes. The measured data are given in Table III. The increasing deviation of the pole frequencies from values after (6) at the lower end of the frequency range can be explained by the increasing passband ripple that has been included in Table III. A realization of the additional coupling α_M in conventional tunable YIG filters should be possible by modification of the design of Fig. 2.

Finally, the effect of the operating temperature on the pole attenuation is shown in Fig. 8. The pole frequencies vary according to the 3-dB bandwidth reduction, as has been described before.

The realization of finite-pole frequencies in a two-stage YIG filter is of interest for applications that require a high rejection only at a small frequency band relatively close to the passband frequency, e.g., for image signal suppression with $|f_p - f_0|$ equal to twice the value of the intermediate frequency, instead of using a three-stage filter.

Acknowledgment

The author wishes to thank Dr. H. Weinerth for his valuable discussions and H. J. Kühn for his help extended in the experiments.

References

[1] G. L. Matthaei, L. Young, and E. M. T. Jones, *Microwave Filters, Impedance Matching Networks and Coupling Structures.* New York: McGraw-Hill, 1964.
[2] R. E. Tokheim and G. F. Johnson, "Optimum thermal compensation axes in YIG and GaYIG ferrimagnetic spheres," *IEEE Trans. Magn.*, vol. MAG-7, pp. 267–276, June 1971.
[3] R. E. Wells, "Microwave bandpass filter design—Part I," *Microwave J.*, vol. 10, no. 11, pp. 92–98, Nov. 1962.
——, "Microwave bandpass filter design—Part II," *ibid.*, vol. 10, no. 12, pp. 82–88, Dec. 1962.
[4] P. S. Carter, "Equivalent circuit of orthogonal-loop-coupled magnetic resonance filters and bandwidth narrowing due to coupling inductance," *IEEE Trans. Microwave Theory Tech.*, vol. MTT-18, pp. 100–105, Feb. 1970.

Computer Analysis of Latching Phase Shifters in Rectangular Waveguide

FRED E. GARDIOL

***Abstract*—Latching phase shifters, consisting of a waveguide section containing a ferrite toroid, are widely used as digital steering elements in microwave array antennas. The theoretical determination of device performance cannot be obtained exactly, since these structures are inhomogeneous along both transverse directions.**

The present study presents an approximate method to evaluate phase shift and losses in the case of a rectangular toroid. An approximately equivalent structure (twin slab), for which an exact resolution method is available, is considered first. The changes due to the upper and lower sections of the toroid are then evaluated by means of a variational principle. Experimental results show good agreement with computed values for several practical cases considered. Finally, the range of validity for this approximate method is determined.

I. Introduction

Ferrite latching phase shifters are major components in modern phased-array radar systems; they generally consist of a rectangular waveguide containing hollow ferrite cylinders magnetized to remanence by means of thin conducting wires. Fig. 1 depicts a widely used configuration, a ferrite toroid of rectangular shape located at the center of the waveguide; the dimensions and the coordinate axes are also indicated on the drawing. The structure is inhomogeneous along both transverse directions $\bar{a}_x$ and $\bar{a}_y$; therefore, an exact analytical resolution for the electromagnetic fields and for the propagation characteristic is not feasible.

The microwave properties of this device can be determined to some extent from the analysis of the twin-slab phase-shifter structure shown in Fig. 2, which is homogeneous along the $\bar{a}_y$ direction. The transverse resonance method can then be used to determine the electromagnetic field distribution and the propagation coefficient [1]–[3]. Results for the twin-slab phase-shifter geometry have been used in the phased-array industry as a first-order approximation to predict the behavior of toroidal devices. However, differences in differential phase shift up to 20 percent or more have been observed between the theory for twin slabs and measurements taken on rectangular toroids. These differences can be either positive or negative; they depend on the material, the geometrical parameters, and the frequency. For instance, if a twin-slab structure is selected to yield a flat phase-shift characteristic versus frequency, this requirement will not be met by the corresponding toroidal device.

Several attempts were made to take into account the effect of the upper and lower sections of the ferrite toroid, leading to a rather amazing situation: for the two approaches published in the literature, the proposed corrections actually have opposite signs! Both of them are apparently based on sound theoretical considerations and

Manuscript received November 8, 1971; revised August 14, 1972.
The author is with the Federal Institute of Technology, Ch. de Bellerive 16, Lausanne, Switzerland.